Indian Journal of Fibre& Textile Research
Vol. 49, September 2024, pp. 318-324
DOI: 10.56042/ijftr.v49i3.12508

Critical characterization of low porosity ripstop parachute canopies using small-scale impact and quasi-static loading principle

Kumari Neha, Monica Sikka[a] & Gyana Ranjan Behera

Department of Textile Technology, Dr B R Ambedkar National Institute of Technology, Jalandhar 144 027, India

Received 24 January 2023; revised received and accepted 16 June 2023

Three levels of maximum sustainable tensile impact load (400, 450 and 500 N) of a small rectangular ripstop parachute canopy specimen stitched at a 45° seam angle have been studied manually. Using the scale-up approach, the proportionate peak sustainable opening shock force for T10, C9, and G11 low porosity canopies have been computed subsequently. This study also characterizes the small rectangular unseamed and seamed specimens at 0° and 45° seam angles under three levels of a maximum sustainable range of tensile impact and quasi-static loads. The ANOVA analysis shows that the fabric seam joining has a greater effect on the specimen's performance than the seam angle and applied load. It is also observed that the specimen degrades significantly more under impact load than the corresponding quasi-static load. Under quasi-static and impact loads, the seamed specimen exhibits more strength and elongation loss than the unseamed specimen. Further, the strength loss for the 0° seam angle is more than the 45° seam angle. The specimen with 45° seam angle exhibits better performance under impact and quasi-static load comparably and exhibits higher loss in elongation but still has higher breaking elongation than the specimen stitched with 0° seam angle at the same load level.

Keywords: Low porosity, Parachute canopy, Ripstop, Seam angle, Impact force, Quasi-static loading, Nylon 66 fabric

1 Introduction

A parachute is a device that slows down a person's vertical descent through the sky. The various parachute components are the pilot chute, slider, suspension line, brake loop, canopy, stabilizer, and harness[1]. The canopy of a parachute is a cloth that decelerates through the air within its structure, generating drag force[2]. Characterization of the parachute canopy is an important aspect of its evaluation before deployment in critical aerodynamic conditions. The parachute canopy is made by joining the number of gores and panels together by stitches and seams and the canopy can be constructed using either a block or a biased method[3]. Figure 1 depicts the structure of gores and panels. The parachute canopies experience different forces during their practical application and the most important is opening shock force, which is developed during parachute deployment. The opening shock force affects the fabric's mechanical properties, like fabric strength and seam strength. Besides the fabric quality, the quality of the seams and stitching, as well as its direction, has an impact on its performance [4-6]. The gore and panels are stitched together with different seam bias angles as per their different applications. The tensile strength of the parachute changes with a change in the bias angle of stitching to warp direction due to the change in orientation of the yarns and the number of yarns gripped between gripping zones[4,6,7]. The study of Coplan and Bloch[8] examined that the 45° bias direction lapped seam gives more efficiency than the orthogonal direction.

To characterize the full-scale or model parachutes, a variety of tests have been used, including a wind tunnel test, aircraft drop test, rocket boost, and extraction test[9]. However, the afore-mentioned tests have several drawbacks, including high complexity, a requirement for extra space, the necessity for skilled operators, and a detailed evaluation of material performance is complicated. Therefore, to overcome these problems, Singh *et al.*[6] studied a small-scale tensile impact testing of the parachute canopy as a small rectangular stitched specimen. Recently, Behera *et al.*[10] developed a method to assess parachute canopy performance under various tensile impact loads.

Numerous studies[4,6,10,11] have been done on the degradation of parachutes under impact loading but there is no prediction about the maximum resistible shock force for different canopies without any damage.

[a]Corresponding author.
E-mail: sikkam@nitj.ac.in

Furthermore, the impact of that maximum resistible shock force on the performance of the canopy using a scale-up approach is not investigated to date.

The present research mainly focuses on the low-porosity ripstop parachute canopies which are widely used for gliding parachutes nowadays. Low-porosity parachute canopies can reduce sink rate and landing injuries[12]. The low-porosity parachutes such as ram-air parachutes, USAF C-9, and US Army T-10/G-12/G-11 personnel and cargo parachutes used in military applications, open very slowly[13]. This study has predicted the maximum resistible opening shock force for low-porosity parachute (C-9, T-10, and G-11) canopies. The dimension of the test specimen has been chosen from earlier research[6]. In this context initially, the dead weights to apply impact and static load on the specimen have been derived based upon the maximum resistible impact force of the specimen seamed at 45° seam angle. Thereafter, the resistible impact force of the specimen is scaled up to determine the maximum resistible opening shock force of the aforesaid canopies. To analyze the performance of the seamed and unseamed specimens, three different peak resistible impact and quasi-static loads have been applied to the specimen. The ANOVA test has been used to measure the contribution percentage of each factor under impact and static loading. Finally, the performance of the specimen has been studied in terms of degradation in breaking strength and breaking elongation.

2 Materials and Methods

2.1 Materials

The low-porosity ripstop nylon fabric [Fig. 2 (a)] was used in this study. The specimen was stitched with nylon 66 sewing thread. The details of the material and sewing thread are shown in Table 1.

2.2 Methods

The different characteristics of the fabric have been assessed (Table 1) as per ASTM standards, such as ASTM D3775-17 for fabric density, ASTM D1059-17 for linear density of warp and weft yarns, ASTM D3883-04 for crimp %, ASTM D3776 for mass density and ASTM D737 for air permeability. The samples are stitched with LSc-2 lapped seam according to ASTM D6193-16, at two different seam angles (0° and 45°), as illustrated in Figs 2 (c) and (d)

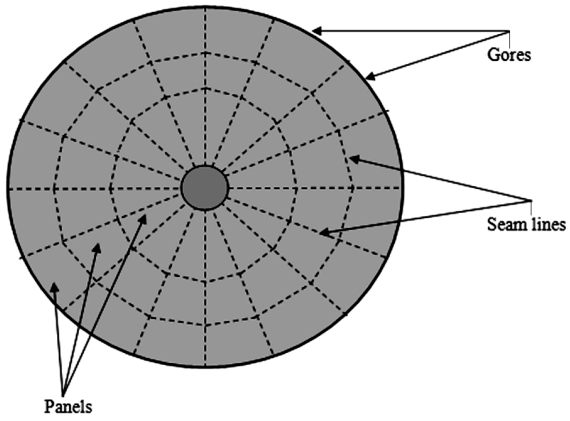

Fig. 1 — Parachute canopy showing gores and panels

Table 1 — Specification of fabric and sewing thread

Fabric type	Ripstop (Nylon 66)
EPI	128
PPI	128
Fabric thickness, mm	0.04
Warp count, tex	3.96 (Finer) 6.88 (Coarser)
Weft count, tex	3.72 (Finer) 7.26 (Coarser)
Warp/Weft crimp, %	1.3/2
Mass density, g/m^2	36.8
Air permeability, cm^3/cm^2/s	0.8
Sewing thread	Nylon 66 (2-ply)
Sewing thread ticket number	40
Stitch density, stitches/cm	3
Distance between two-seam, mm	10

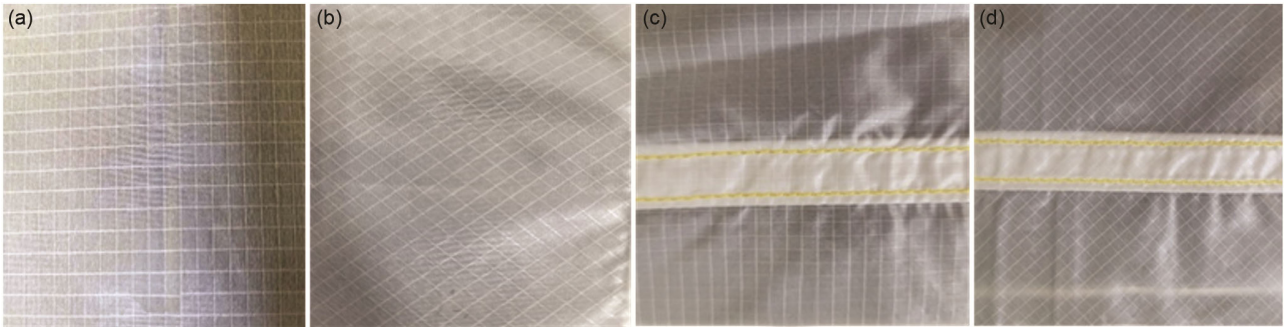

Fig. 2 — Images of unseamed specimens at (a) 0° angle and (b) 45° bias angle, with the fabric orientation/angle; seamed specimens at (c) 0° seam angle and (d) 45° seam bias angle with the fabric orientation/angle

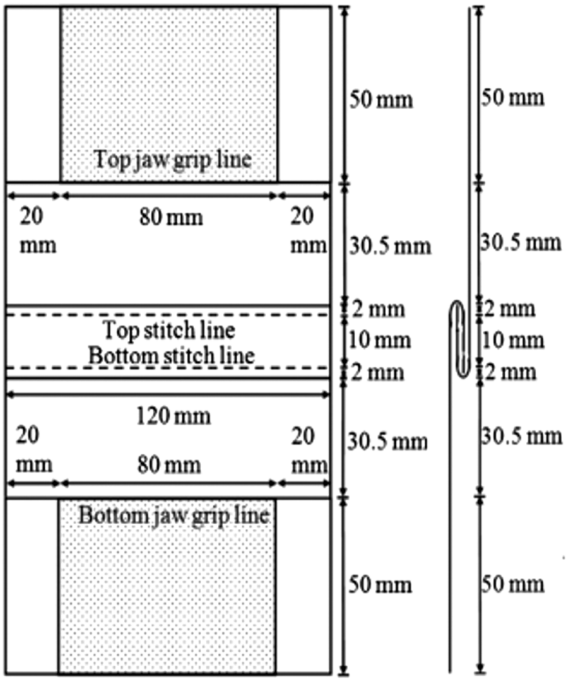

Fig. 3 — Grab test specimen dimension and its side view for measurement of tensile and impact loading[6]

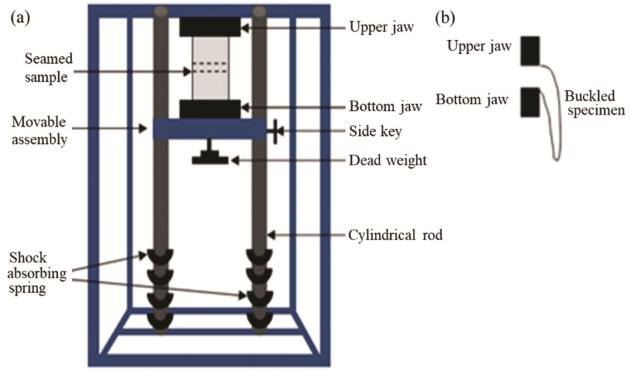

Fig. 4 — (a) Fabric tensile impact tester and (b) specimen in folded configuration

respectively. Figures 2 (a) and (b) illustrate the unseamed samples.

The specimen's dimension (Fig. 3) for small-scale tensile impact testing is used in the present study, which is taken from the earlier research where the fabric sample is stitched by using LSC-2 lapped seam[6].

2.3 Application of Impact and Quasi-static Load

A prefabricated tensile impact tester (Fig. 4) is used for the application of impact load[6]. A CRE-tensile tester is used to apply quasi-static load on the specimen and also used to evaluate the residual tensile strength and elongation of the specimen.

2.4 Selection of Load for Impact Loading

The impact load on the specimen can correlate with the opening shock force of the canopy. The level of impact load on the fabric specimen varies with the dead weight, which has been determined manually. In this case, the widely used seam angle for parachute canopy stitching, (45° seam angle) is used to prepare the specimen and is performed under tensile impact load using pre-fabricated tensile impact tester and different dead weights. The experimented dead weight ranged from 1 kg to continuously rising by 0.5 kgf, and it was found that the specimen breaks at a dead weight of 8.5 kgf while resisting the maximum impact load by a dead weight of 8 kgf. Since the aim of the present study is also to analyze the effect of the specimen under the 3 levels of a maximum sustainable range of tensile impact loads, the 3 levels of dead weight (8 kg, 7 kg, and 6 kg) and corresponding impact loads 500 N, 450 N, and 400 N were selected. The impact force is calculated by using the given equation:

$$F = \frac{mg\,(h+d)}{d} \qquad \ldots(1)$$

where m is the dead weight provides an impact load (kg); g, the acceleration due to gravity (9.81m/s^2); h, the length of the specimen (m); and d, the extension of specimen during impact (m).

2.5 Selection of Load for Quasi-static Loading

The quasi-static loading on the specimen can correlate with the parachute canopy at the time of steady descent. The 3 levels of quasi-static loads to be applied on the specimen are selected based on the afore-said impact loads (400 N, 450 N and 500 N).

2.6 Experimental Design and Contribution Percentage

In this study, a total of 12 specimens were investigated where the 3 replications were used for each specimen. The experimental design was based on the seam joining of the specimen (seamed and unseamed), seam angles (0° and 45°), and load (400 N, 450 N, and 500 N). The contribution percentage of each factor on breaking strength and breaking elongation has been determined using ANOVA results, as per the formula given below:

Contribution % due to any particular factor (suppose S)=

$$\frac{SS_S - (df_S \times MSE_P)}{SS_T} \times 100 \qquad \ldots(2)$$

where SS_S is the sum of squares due to any factor (suppose S); df_S, the degree of freedom due to any

factor (suppose S); MSE_P, the mean squared prediction error [(residual SS)/ (residual df)]; and SS_T, the total sum of square.

3 Results and Discussion

3.1 Prediction of Maximum Resistible Opening Shock Force for Low Porosity Canopies

The parachute may experience higher opening shock force in critical aerodynamic circumstances and may be used for different heavy loads applications, such as military equipment and ammo droppings where the chance of structural failure of the canopy is very high. Thus, the prediction of maximum resistible opening shock force by the canopy is essential and in the present study, the T10, C9, and G11 low porosity parachute canopies are selected for the prediction. The mathematical formula for the estimation of the maximum resistible opening shock force on the parachute canopy is given below:

Let's assume that the maximum resistible opening shock force on the canopy is F_{max}, which is shared through the entire circumference of the canopy. Using a scale-down approach, the shock force through the unit width of the canopy is,

$$\frac{F_{max}}{\pi D_P} \quad \ldots(3)$$

where D_P is the projected diameter (m) of the canopy; and for a flat circular parachute, it is approximately given by[14]

$$D_P = D_o \times C_d \quad \ldots(4)$$

where C_d is the drag co-efficient of a parachute; and D_0, the opening diameter of the parachute.

Since the present specimen consists of 80 mm width, the stress on the specimen can be represented as,

$$S_{max} = \frac{F_{max}}{\pi D_P} \times 0.08 \quad \ldots(5)$$

Using the reverse scale-down approach, the maximum resistible opening shock force is,

$$F_{max} = \frac{S_{max} \times \pi D_p}{0.08} \quad \ldots(6)$$

Now, F_{max} is considered as the maximum resistible opening shock force on the parachute canopy; while S_{max} is the maximum resistible impact force on the specimen.

In the present study, considering the scale-down approach, a small stitched low porosity ripstop specimen is prepared and subjected to different levels of tensile impact force produced by different dead weights. The experimented maximum resistible tensile impact load has been determined as 500 N. Thereafter, using Eq. (6) or the reverse scale-down approach of the test specimen, the maximum resistible opening shock force on the canopy is computed. The specifications along with the computed resistible opening shock forces of the T10, C9, and G11 canopies are given in Table 2. The G11 parachute canopy shows a greater resistible opening shock force as compared to T10 and C9 parachute canopies due to a higher corresponding opening diameter and projected diameter.

3.2 ANOVA Analysis

The change in tensile properties of stitched and unstitched ripstop fabric has been analyzed after the applications of three levels of impact loads and quasi-static loads (with load values of 500 N, 450 N, and 400 N for each). Three-way ANOVA has been used to measure each factor's contribution percentage on the change in breaking strength and elongation of the specimen (Table 3).

The role of seam joining (seamed/unseamed) is higher on the specimen's breaking strength than on the seam angle and loads under both impact and quasi-static loadings. The role of impact and quasi-static loads on breaking strength is less significant than other factors. Further, the interaction among all input variables on the breaking strength is small/ insignificant. The effect of seam angle (0° seam angle/ 45° bias seam angle) is higher on breaking elongation of the specimen under both impact and quasi-static loadings than load and seam joining. Moreover, the interaction between different variables on the breaking elongation of the specimen is less or has no significant effect. A detailed description of output parameters is given in the subsequent sections.

Table 2 — Calculated maximum resistible opening shock force along with the specification of different low-porosity parachute canopies[10,15,16]

Parachutes	Opening diameter (D_o), m	Drag co-efficient (C_d)	Projected diameter ($D_p = D_o \times C_d$), m	Maximum resistible opening shock force (F_{max}), N
T 10	7.3	0.7	5.11	100283.75
C 9	8.5	0.7	5.95	116768.75
G 11	10.7	0.7	7.49	146991.25

3.3 Effect of Impact Load on Tensile Characteristics of Ripstop Parachute Fabric Specimen

During parachute opening, it experiences a sudden impact force which continuously deteriorates the tensile properties of the fabric. To analyze this degradation, the specimen is subjected to three levels of impact loading (400, 450 and 500 N), and the loss in breaking strength and breaking elongation of the specimen is measured. It has been observed that after the impact loading, the specimen's breaking strength and elongation decrease.

3.3.1 Change in Breaking Strength of Specimen

Figure 5 (a) shows that as the impact load (preload) increases, the loss in breaking strength increases. Here, zero preload means no impact load has been exerted onto the specimen. With an increase in dead weight, the specimen's impact load and the related opening shock force on the parachute canopy will increase, which results in more strength loss. In addition, the degradation in the specimen with 0° fabric angle is more as compared to the specimen with 45° fabric bias angle. This is primarily due to the completely symmetric alignment of warp-weft yarns in the specimen with 45° bias fabric angle, and both warp-weft yarns equally bear the applied stress and also absorb more force due to higher elongation[6].

The seamed specimen shows a higher loss in breaking strength than the unseamed specimen. Also, most of the specimen's breakage is discovered near the seam. It means that the properties of the sewing thread affect the breaking strength of the seamed fabric.The specimen with 0° seam angle exhibits more breaking strength loss as compared to the specimen with 45° bias seam angle. In the case of the specimen with 0° seam angle, the seam line can be considered as a secondary jaw. Hence, when force is applied then this creates a hole near the seam line which ultimately leads to the breakage of the specimen. The specimen with 45° bias seam angle has less breaking strength loss due to a greater number of yarns gripped within both primary jaws and the seam line, which can be considered a secondary jaw that prevents the free yarn from slipping out during the specimen's tensile test[6]. Further, the effect of preload is similar to unseamed specimens. The loss in breaking strength for 0° seamed specimen at 500 N is 100% as it breaks under the tensile impact load, as also indicated in Fig. 5 (a).

Table 3 — Contribution % of different parameters on tensile properties of specimen during impact and quasi-static loadings

Parameters	% of Contribution			
	Breaking strength, N		Breaking elongation, %	
	Impact	Quasi- static	Impact	Quasi- static
Load	10.09	9.12	7.3	7.43
Seam joining	47.49	50.24	9.29	7.2
Angle	15.17	15.88	72.97	74.03
Load *vs* seam	7.55	6.88	4.95	3.38
Load *vs* angle	7.69	-	0.94	-
Seam *vs* angle	-	-	-	-

(-) indicates the insignificant at 0.05 significance level and negligible % of the contribution.

3.3.2 Change in Breaking Elongation of Specimen

The graph between preload and loss in breaking elongation is plotted in Fig. 5 (b) among 0° and 45° fabric angles for both unseamed and seamed specimens. The loss in breaking elongation increases with an increase in preload. It is clear that the specimen with 45° fabric angle has more loss in breaking elongation than the specimen with 0° bias fabric angle, but still has higher breaking elongation at the same preload level. The yarns inside the specimen with 0° fabric angle have very less load sharing time during impact and cause load imbalance, hence less breaking elongation. At 45° bias angle,

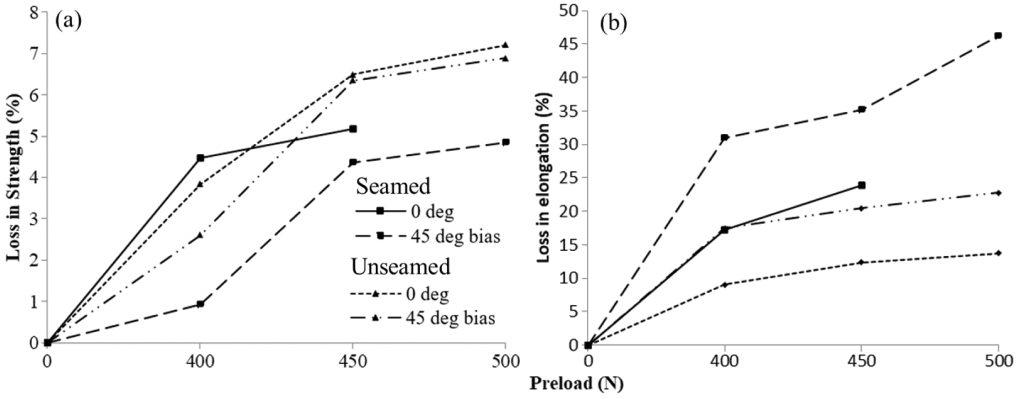

Fig. 5 — Effect of impact load on loss in (a) breaking strength and (b) breaking elongation of seamed and unseamed specimens with 0° and 45° seam/fabric bias angle

yarn symmetry dominates and supports the warp and weft yarns in load distribution, resulting in higher breaking elongation.

Also, the loss in breaking elongation is greater for seamed fabric as compared to unseamed fabric due to the properties of the sewing thread and the seam line. The breaking elongation loss increases with an increase in preload during impact. Figure 5 (b) clarifies that the loss in breaking elongation for the 0° seamed specimen at 500 N is 100% when it breaks under the tensile impact force.

3.4 Effect of Quasi-static Load on Tensile Characteristics of Ripstop Parachute

The quasi-static load is exerted onto the parachute canopy at the time of steady descent. The quasi-static load also degrades the tensile characteristics of the parachute canopy. The specimen is subjected to quasi-static load on a CRE-based UTM and then degradation of the tensile characteristics has been analyzed. It has been observed that the breaking strength and the breaking elongation of the specimen decrease after the quasi-static loading.

3.4.1 Change in Breaking Strength of Specimen

It has been revealed that the quasi-static loading also degrades the specimen but to a lesser extent. According to the force equation (force = mass × acceleration), impact loads have a higher shock on fabric than quasi-static loads. An increase in force also results from abrupt deceleration. Quasi-static loads exert less force than impact loads. Therefore, impact loading causes more loss than static loading[17].

The preload vs loss in breaking strength of unseamed specimens at 0° and 45° fabric bias angles along with seamed specimens at 0° and 45° bias seam angles under quasi-static load is plotted in Fig. 6(a). The loss in breaking strength of the seamed and unseamed specimens with 0° seam and fabric angles respectively is greater than the corresponding 45° seamed and unseamed specimens as discussed above. The specimen with a 0° seam angle exhibits more breaking strength loss as compared to the specimen with a 45° bias seam angle. In the case of the 0° seam angled specimen, the seam line is perpendicular to the warp yarns and during the application of force (preload), the warp yarns inside the seam lines can easily slide out/loosen from the needle holes of the gripped sewing threads. This causes to more loss in the stregth due to preload for 0° seam angled specimen. Conversely, the specimen with a 45° bias seam angle experiences less breaking strength loss because more yarns are gripped between the two primary jaws along with the the seam line, and the yarns are oriented angularly to the respective jaw lines. These orientations of the yarns preventing from slipping out during the preload or tensile test of the specimen. Additionally in the results, it is noticed that the extent of loss in breaking strength during quasi-static load is less than the loss in breaking strength during impact load. The seamed specimen shows a higher loss in breaking strength than the unseamed specimen. It means that the needle holes during to stitching operation affect the breaking strength of the seamed fabric. The loss in breaking strength for 0° seamed specimen at a preload of 500 N is 100% as it breaks under 500 N load.

3.4.2 Change in Breaking Elongation of Specimen

The contribution % of seam angle specimen affects the specimen's breaking elongation more than other factors during quasi-static loading (Table 3). The loss

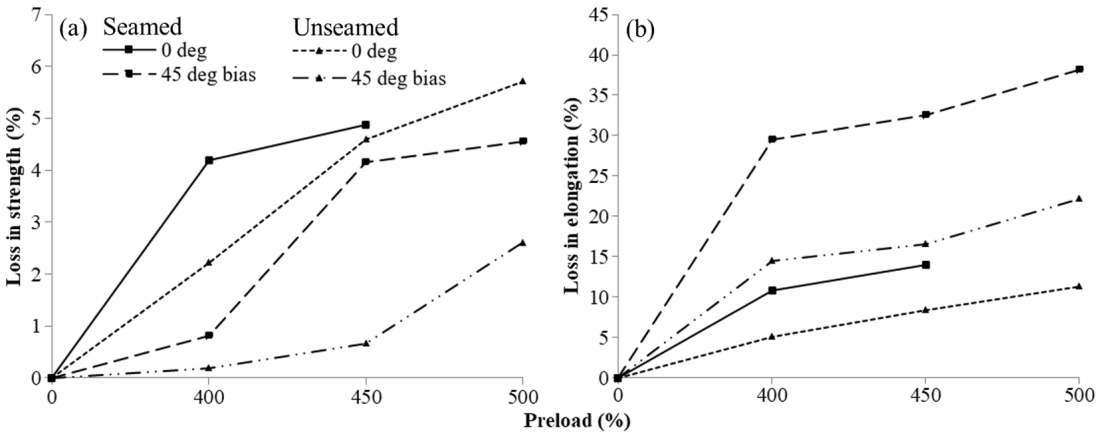

Fig. 6 — Effect of quasi-static load on loss in (a) breaking strength and (b) breaking elongation of seamed and unseamed specimens with 0° and 45° seam/fabric bias angle

in breaking elongation has been measured for seamed and unseamed specimens. Impact-loaded specimens exhibit a continuous decrease in breaking elongation, similar to tensile strength behaviour.

The effect of quasi-static load on the degradation in breaking elongation of the unseamed samples at 0° and 45° fabric bias angles along with seamed specimens at 0° and 45° bias seam angles under quasi-static load are indicated in Fig. 6 (b). It is noticed that both seamed and unseamed specimens with a 45° bias seam and fabric angles respectively show more loss in breaking elongation than the specimen with a 0° seam and fabric angle. The threads in the specimen with a 45° bias fabric angle are diagonally orientated across the fabric, resulting in maximum length and more extension during stretching, as well as adequate recovery. On the other hand, in the case of a 0° seam/fabric angle, the extension is less, and the recovery length is less. However, the percentage of recovery is higher in the 0° specimen when compared to the 45° seam/fabric angle. The aforesaid statement can justify that the specimen with 45° has more loss in breaking elongation than the specimen with 0° fabric/seam angle.

Furthermore, the loss in breaking elongation is more for seamed fabric as compared to unseamed fabric due to the needle holes near the seam line as discussed earlier. The sewing or joining process can produce a localized yarn displacement, yarn damage, or altered yarn orientations at the seam line. It is demonstrated from Fig. 6 (b) that the 0° seamed specimen loses 100% of its tensile strength along with elongation as it breaks under 500 N load.

4 Conclusion

The study reveals that the maximum resistible opening shock force for low porosity parachute canopies T10, C9, and G11 are 100283.75 N, 116768.75 N, and 146991.25 N respectively. It has been investigated using the ANOVA test that the seam joining of the fabric has the highest contribution to the performance of the parachute canopy than the seam angle and the load. The specimen degrades more under impact load in comparison to the corresponding quasi-static load. The specimen stitched with 0° seam angle shows more degradation and may lead to canopy failure at high impact opening shock force, whereas the specimen stitched with 45° bias seam angle has less degradation because of higher breaking elongation. It can be concluded that the specimen stitched at a 45° bias seam angle exhibits better performance under both impact and quasi-static load and it may be the preferable option for parachute canopy construction over a 0° seam angle.

References

1 Cockrell D J & Young A D, *The Aerodynamics of Parachutes* (Advisory Group for Aerospace Research and Development, United Kingdom), 1987.

2 Canbolat F M, *Electronic J Text*, 5 (2011) 72.

3 Design and Construction*, Handbook Parachute Rigger* (U.S. Department of Transportation, Federal Aviation Administration, Airman Testing Standards Branch, AFS-630 Oklahoma City, USA), 2005, 1.

4 Mukhopadhyay A, Chatterjee A & Singh H, *J Industrial Text*, 46 (2016) 320.

5 Mukhopadhyay A & Midha V K, in *Joining Textiles*, edited by I Jones & G K Stylios (Woodhead Publishing Cambridge, UK) 2013, 175.

6 Singh H, Mukhopadhyay A & Chatterjee A, *J Text Inst,* 108 (12) (2017) 2057.

7 Mukhopadhyay A, Chatterjee A & Ahuja T, *Text Light Industrial Sci Technol*, 3 (2014) 29.

8 Coplan M L & Bloch M G, *Wright Air Development Centre Technical Report* (Defense Technical Information Center), (1956) 56.

9 Jodehl J W, Anton S V, Bosboom T C, Dhiyaneeswaran S, Dvorak O, Homola M, Knoll N, Menting E & Sujahudeen M S, *Architectures for Parachute Testing,* paper presented at the 72nd International Astronautical Congress, Dubai UAE*,* 25-29 October 2021.

10 Behera G R, Mukhopadhyay A & Sikka M, *J Industrial Text*, (2022) 1.

11 Behera G R, Sikka M & Mukhopadhyay A, *J Text Inst*, (2022) 1.

12 Bagian J P,*Aviat Space Environ Med*, 63 (1992) 802.

13 McQuilling, Jean Potvin & Mark, *The Bi-Model: Using CFD in Simulations of Slowly Inflating, Low-Porosity Hemispherical Parachute,* paper presented at the 21st AIAA Aerodynamic Decelerator Systems Technology Conference, and Seminar,Dublin, Ireland, 23-26 May 2011.

14 Solt GC, *AF Flight Dynamics Laboratory Research and Technology Division* (American Power Jet Co., Ridgefield, New Jersey), 1963, 374.

15 https://www.millsmanufacturing.com/products/t-10r-parachute/, (assessed on 10/08/2022).

16 https://www.millsmanufacturing.com/products/g-11-parachute/, (assessed on 10/08/2022).

17 https://www.twi-global.com/technical-knowledge/faqs/what-is-static-loading, (assessed on 07/06/2022).